Article:
Skowron, ST, Chamberlain, TW orcid.org/0000-0001-8100-6452, Biskupek, J et al. (3 more authors) (2017) Chemical Reactions of Molecules Promoted and Simultaneously Imaged by the Electron Beam in Transmission Electron Microscopy. Accounts of Chemical Research, 50 (8). pp. 1797-1807. ISSN 0001-4842

https://doi.org/10.1021/acs.accounts.7b00078

Accounts of Chemical Research (6,000 words).

Chemical Reactions of Molecules Promoted and Simultaneously Imaged by the Electron Beam in Transmission Electron Microscopy

Stephen T. Skowron,[a] Thomas W. Chamberlain,[a,b] Johannes Biskupek,[c] Ute Kaiser,[c] Elena Besley,[a] Andrei N. Khlobystov*[a,d]

[a] *School of Chemistry, University of Nottingham, NG7 2RD Nottingham, UK*

[b] *Institute of Process Research and Development, School of Chemistry, University of Leeds, Leeds, LS2 9JT, UK*

[c] *Central Facility of Electron Microscopy, Electron Microscopy Group of Materials Science, University of Ulm, 89081 Ulm, Germany*

[d] *Nanoscale & Microscale Research Centre, University of Nottingham, University Park, NG7 2RD, UK*

* andrei.khlobystov@nottingham.ac.uk

Conspectus

The main objective of this Account is to assess the challenges of TEM of molecules, based on over 15 years of our work in this field, and to outline the opportunities in studying chemical reactions under the electron beam (e-beam). During transmission electron microscopy (TEM) imaging of an individual molecule adsorbed on an atomically thin substrate, such as graphene or a carbon nanotube, the electron beam (e-beam) transfers kinetic energy to atoms of the molecule, displacing them from equilibrium positions. The impact of e-beam triggers bond dissociation and various chemical reactions which can be imaged concurrently with their activation by the e-beam and can be presented as stop-frame movies. This experimental approach, that we term *ChemTEM*, harnesses energy transferred from the e-beam to the molecule via direct interactions with the atomic nuclei, which enables accurate prediction of bond dissociation events and control of the type and rate of chemical reactions. Elemental composition and structure of the reactant molecules, as well as the operating conditions of TEM (particularly energy of the e-beam) determine the product formed in *ChemTEM* process, while e-beam dose rate controls the reaction rate. Because the e-beam of TEM acts simultaneously as a source of energy for the reaction and as an imaging tool monitoring the same reaction, *ChemTEM* reveals atomic-level chemical information, such as pathways of reactions imaged for individual molecules, step-by-step and in real time; structures of illusive reaction intermediates; and direct comparison of catalytic activity of different transition metals filmed with atomic resolution. Chemical transformations in *ChemTEM* often lead to previously unforeseen products, which demonstrate the potential of this method to become not only an analytical tool for studying reactions, but also a powerful instrument for discovery of materials that can be synthesised on preparative scale.

Introduction: molecules in electron beam

Sub-Angstrom resolution has been achieved in transmission electron microscopy (TEM) at the turn of the century due to the significant progress in aberration correction technology. As a result, structures of molecules can now be imaged with atomic resolution, at least in principle. However, in

practice imaging of molecules with atomic resolution is extremely difficult because the quality of TEM data is *not limited by the resolution of the instrument but rather by the stability of the molecules under the e-beam*. It is not a coincidence that one of the first and most studied molecules by TEM is the fullerene C_{60} – a highly stable species with three strong covalent bonds for each carbon atom and no edges (Figure 1). Early work on TEM imaging of C_{60} and other fullerenes stimulated development of low-voltage TEM (LV-TEM). In particular, the aberration-corrected TEM developed in the framework of the SALVE project enables imaging with electron energies in the range between 80keV and 20keV (www.salve-project.de, [1,2]).

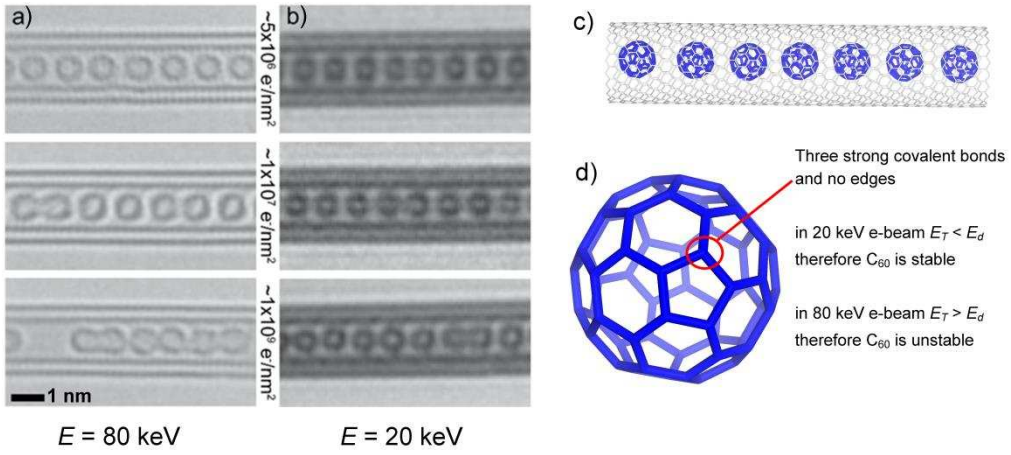

Figure 1. e-Beam dose-series TEM images of C_{60} fullerenes in carbon nanotubes show a much greater stability of the molecules under 20 keV (b) than 80 keV (a) e-beam. (d) Fullerenes inserted into a carbon nanotube (c) C_{60}@SWNT are useful for studying e-beam – molecule interactions.

Whenever TEM is applied to characterisation of molecular materials, atoms of the molecules are engaged in interactions with fast electrons of the e-beam, so that molecules during TEM investigation always receive energy either due to e-beam interactions with electrons of the atoms or e-beam interactions with the atomic nuclei. Distinction between these two mechanisms of e-beam – molecule interactions is crucially important for understanding the impact of TEM on molecules, and thus it is instructive to assess how these mechanisms depend on experimental conditions.

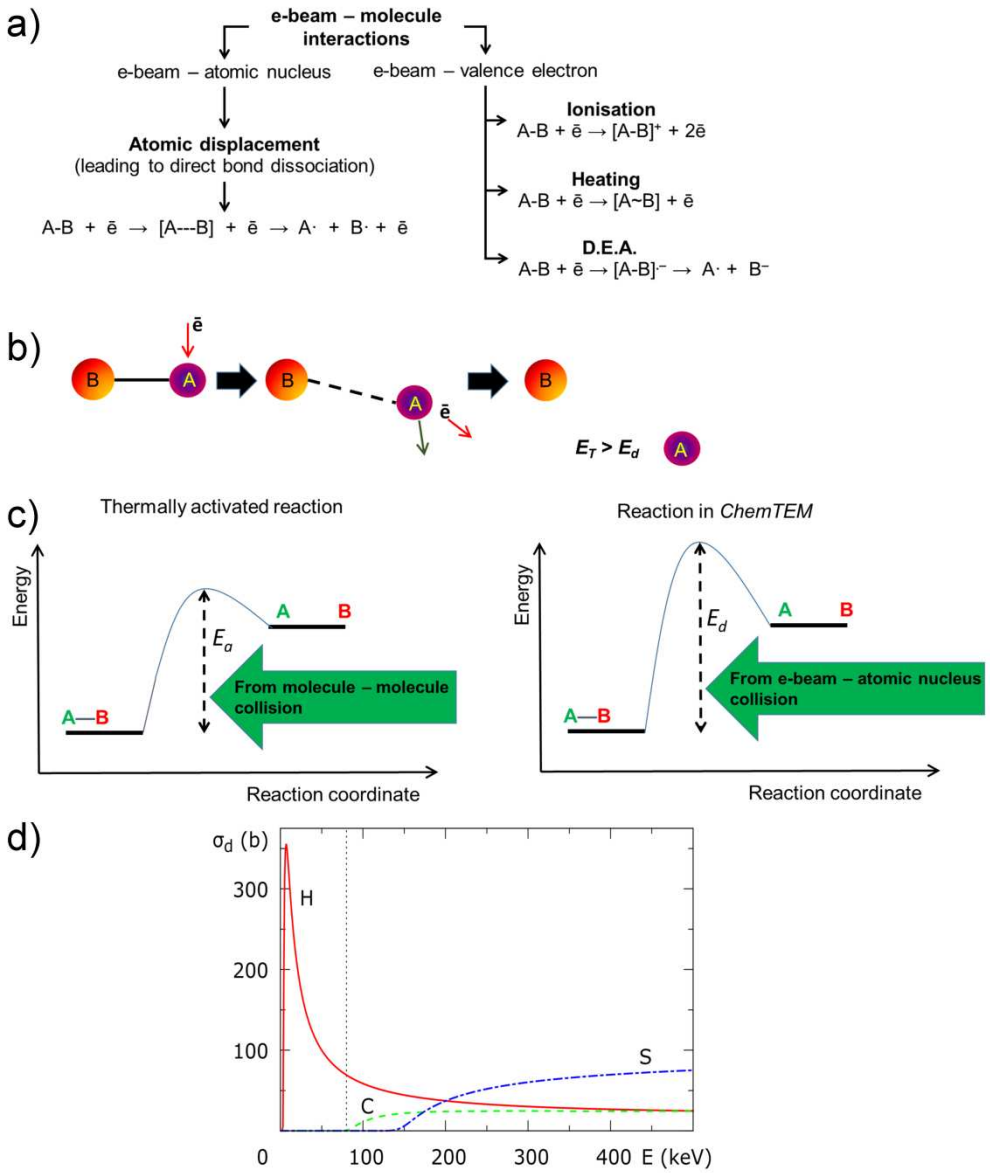

Figure 2. (a) Types of e-beam – molecule interactions depend on the energy of the e-beam and the configuration of the sample. (b) E-beam interaction with the atomic nucleus causes displacement of the atom from its equilibrium position and, if the transferred energy is sufficiently high, dissociation of the chemical bond. (c) Energy to promote a chemical reaction in *ChemTEM* is supplied by collisions between the individual molecule and incident electrons, whereas in traditional chemical reactions the activation energy originates from intermolecular collisions. (d) Cross section σ_d describes the likelihood of atom displacement from a specific chemical bond (C-H, red plot; aromatic C-C, green plot; C=S blue plot) as a function of the e-beam energy.

E-beam – atomic electron interactions are prevalent when a low energy e-beam, such as the 0.01-1 keV e-beam applied for cross-linking organic molecules in self-assembled monolayers, or when a high energy e-beam interacts with a thick molecular material (e.g. thicker than a monolayer), such as the 30-80 keV e-beam in electron beam lithography (EBL) of polymeric films. As the high energy e-beam penetrates deeper into the material, it undergoes multiple interactions with atoms of the molecules, and the initially fast incident electrons progressively lose their energy and slow down while generating a large number of secondary, lower energy electrons, with the latter being a particularly important process for transformations of molecules in the EBL. These lower energy secondary electrons have a

high probability (quantified as a cross section) for interactions with molecular orbitals, either knocking out further valence electrons or undergoing dissociative electron attachment (DEA) with anti-bonding molecular orbitals, when their kinetic energy approaches zero. Therefore, in processes such as EBL or in TEM experiments with thick molecular samples e-beam – atomic electron interactions are dominant and the amount of energy transferred from the primary e-beam to the valence electrons of the molecules, E_T, is described as ,

$$E_T(b) = e^4/(4\pi\cdot\varepsilon_0)^2 E\cdot b^2 \quad \text{Equation 1}$$

where *e* is the charge of an electron, *b* is the distance between the incident and valence electrons, ε_0 is the permittivity of free space, *E* is the energy of the primary e-beam. These interactions trigger numerous secondary effects, such as the emission of X-rays, or heating of the material, as well as causing C-H bond cleavage followed by cross-linking of the neighbouring molecules in the polymer film. It is estimated that ~80% of e-beam damage to organic films (e.g. 100 nm thick PMMA at *E* = 100 keV) is due to secondary electrons [3].

In stark contrast, an isolated molecule or a number of discrete molecules, in vacuum or deposited on a very thin substrate such as graphene or in a single-walled carbon nanotube (SWNT), experience very different effects of the e-beam of the TEM. When the material effectively has no bulk volume, impact of secondary electrons is limited, which in conjunction with drastic reduction in the number of nearest neighbours, limits interactions to the primary electron beam transferring momentum directly onto atomic nuclei. The amount of energy transferred, E_T, from the e-beam to a stationary atom in this case is described as

$$E_T(\theta) = \frac{2m_n E(E+2m_e c^2)}{(m_n+m_e)^2 c^2+2m_n E} sin^2\left(\frac{\theta}{2}\right) = E_{T\_max} sin^2\left(\frac{\theta}{2}\right) \quad \text{Equation 2}$$

where m_n is the mass of the atom and θ is the electron scattering angle. In addition, the SWNT and graphene possessing excellent thermal and electrical conductivities, effectively mitigate heating and ionisation. Overall, in contrast to e-beam – atomic electron interactions (equation 1), the energy transferred to molecules in a e-beam – atomic nucleus interaction is directly proportional to the energy of the e-beam, *E* (equation 2), which means that the stability of molecules can be improved by decreasing the energy of the e-beam, as demonstrated for fullerenes (Figure 1) [2].

Direct stimulation of reactions in molecules by the electron beam in TEM

Whether desired or not, the e-beam interacts with molecules during TEM imaging and transfers a fraction of its momentum to atoms, which causes the atoms to shift from equilibrium positions within the molecule. If the maximum energy that can be transferred from a single electron to an atomic nucleus, E_{T_max} (when $\theta = 180^o$), exceeds the threshold energy (E_d) for a particular chemical reaction, for example a bond dissociation (Figure 2b), the molecule breaks down under the e-beam. If interactions between the e-beam and the molecule are fully understood, any structural changes promoted by the e-beam can be viewed as chemical reactions that shed light on dynamic and chemical properties of the molecules under investigation. In fact, the e-beam of the TEM can readily be employed for a dual purpose: *as a source of energy delivered to the molecule and simultaneously as a probe providing images of the same molecule*. A voltage-tuneable aberration corrected TEM, such as the SALVE instrument with *E* = 20-80 keV [1,2], could give an unprecedented opportunity to observe the molecules reacting and interacting, in direct space and real time, while supplying kinetic energy to the atoms in a controlled manner. Previous attempts to advance temporal resolution of TEM included

correlated laser beam and e-beam pulses in so-called 4D TEM, but this had a detrimental impact on the spatial resolution thus precluding studying of individual molecules [4]. In contrast, the concept of simultaneous use of the e-beam as an energy pump for reactions *and* as an imaging probe to follow them at the single-molecule level opens up an entirely new methodology to study chemistry of molecules by TEM, which we term *ChemTEM*. Within the framework of *ChemTEM* we can tame so-called 'electron beam damage' which is usually seen as the ugly face of TEM, as a new tool for studying molecular reactivity.

Most molecules consist of different types of atoms and bonds, which exhibit different reactivity under the e-beam. Hence it is essential to ascertain the probability of a particular reaction taking place in TEM. The rate of the reaction is quantified by the rate constant *k*, which for a single molecule is only dependent on the cross-section σ of the reaction and the electron dose rate *j* (in electrons/s·nm^2). The time period *t* before the reaction occurs (the lifetime of the molecule under the e-beam) is simply:

$$t = \frac{1}{k} = 1/j\sigma \qquad \text{Equation 3}$$

j is readily and directly controlled by the experimental settings of the TEM, while σ is dependent on *E* and so must be assessed for each e-beam energy. This presents a challenge as the typical velocity of an electron in TEM measurements is an appreciable fraction of the speed of light (e.g. 0.5c at 80 keV), the Rutherford cross-section, σ_R (equation 4), is unsuitable as it neglects of the effects of relativity and electron spin. Instead, the Dirac wave equation must be solved using the Mckinley-Feshbach approximation which modifies the Rutherford cross-section, σ_R, to a cross-section function, $\sigma(\theta)$ (equation 5), more suitable for TEM:

$$\sigma_R = \left(\frac{Ze^2}{4\pi\varepsilon_0 \cdot 2m_e \cdot c^2}\right)^2 \frac{1-\beta^2}{\beta^4} \csc^4\left(\frac{\theta}{2}\right) \qquad \text{Equation 4}$$

$$\sigma(\theta) = \sigma_R \left[1 - \beta^2 \sin^2\frac{\theta}{2} + \pi \frac{Ze^2}{\hbar c}\beta \sin\frac{\theta}{2}\left(1 - \sin\frac{\theta}{2}\right)\right] \qquad \text{Equation 5}$$

where Z is the nuclear charge, β is the electron velocity as a fraction of the speed of light, c. This approximation is comparable to the exact solution for all chemical elements with an atomic number lower than nickel (Z = 28), while for heavy atoms, such as gold, it performs worse than even the Rutherford cross-section. Rewriting the cross-section in terms of the transferred energy (E_T) and integrating in the energy domain where the energy transferred to the atom from the e-beam is greater than the threshold energy of the reaction ($E_T > E_d$) yields an expression describing the cross-section of an e-beam induced reaction, σ_d,:

$$\sigma_d = 4\pi \left(\frac{Ze^2}{4\pi\varepsilon_0 \cdot 2m_e \cdot c^2}\right)^2 \frac{1-\beta^2}{\beta^4} \left\{\frac{E_{T\_max}}{E_d} - 1 - \beta^2 ln\left(\frac{E_{T\_max}}{E_d}\right) + \pi \frac{Ze^2}{\hbar c}\beta \left[2\left(\frac{E_{T\_max}}{E_d}\right)^{1/2} - ln\left(\frac{E_{T\_max}}{E_d}\right) - 2\right]\right\}$$

Equation 6

which can be used to predict rates of reactions in *ChemTEM* using equation 3 [5].

An additional correction may be required due to the thermal energy of the molecule, as the atoms are not stationary during the electron collision, which can increase the maximum transferred energy at a given e-beam energy (equation 2). These thermal vibration contributions to the cross-sections are

calculated from a Maxwell-Boltzmann distribution at 298 K, and the energy transferred from the incident electron to the atom is simply added to the existing velocity of the atom due to the bond vibrations at 298 K. As the interaction of the e-beam with the atom is extremely quick (in the order of approximately 10^{-22} seconds), the dynamics of the system comply with the Born-Oppenheimer principle, enabling the prediction of the reaction outcome via molecular dynamics simulations. This therefore provides a simple physical framework for understanding the reactivity of molecules under the e-beam that can be correlated with *ChemTEM* observations.

The problem of C-H bonds

The weight of the atom, the strength of bonding of the atom and the energy of the e-beam are three key parameters that determine σ_d and, therefore, the reaction rate of that atom in the e-beam (equation 3). It is conventional to plot cross section, σ_d, against the energy of the e-beam, controlled by the accelerating voltage of the TEM instrument (Figure 2d). The plot $\sigma_d(E)$ can be useful to predict under which operating conditions of the TEM a particular atom cannot be displaced from the molecule (i.e. when a chemical bond is unreactive, $\sigma_d = 0$), or when the atom is displaced either with a moderate rate so that this process could be captured by TEM imaging (σ_d ~ 1-10 barn) or so fast such that the molecule decomposes instantaneously under the e-beam ($\sigma_d >> 10$ barn). For example, $\sigma_d(E)$ plots for an aromatic C-C and a C=S bonds show that both bonds can be activated and broken by the e-beam of energy above 150 keV, which means that for TEM to be used for structural analysis of a molecule containing such bonds, the microscope should be operated with an e-beam energy below 80 keV; but if reactions of these bonds are desired with rates commensurate with TEM imaging, the e-beam should be in the range of 90-150 keV. A general rule of thumb, provided that all other parameters are the same, can be stated as follows: (i) molecules with weaker bonds will be more reactive under the e-beam than those with stronger bonds (lower $E_d \rightarrow$ higher $\sigma_d \rightarrow$ higher k); (ii) molecules consisting of heavier atoms will be less reactive than those consisting of lighter atoms (higher $m_n \rightarrow$ lower $E_T \rightarrow$ lower $\sigma_d \rightarrow$ lower k); (iii) under an e-beam of higher energy most chemical bonds within a molecule (with one very important exception) will be more reactive than under an e-beam of lower energy (higher $E \rightarrow$ higher $E_T \rightarrow$ higher $\sigma_d \rightarrow$ higher k).

Unfortunately, this convenient and simple logic appears to break down in the case of chemical bonds containing hydrogen. For example, the σ_d function for C-H bond disobeys the usual $\sigma_d(E)$ trend since the likelihood of C-H bond dissociation increases sharply as the energy of the e-beam decreases below 100 keV (Figure 2d). As experimentally demonstrated by isotope exchange of protium for deuterium [6], the highly labile behaviour of hydrogen under the e-beam is due to the exceptionally low atomic weight of hydrogen (m_n = 1), as compared to other common elements (e.g. carbon or heavier elements), which causes a large amount of energy, E_T, to be transferred from the e-beam to hydrogen (equation 2). Despite the fact that the Rutherford scattering cross section (equations 4 and 5) is always lower for hydrogen (Z = 1) than for other elements, the overall cross section, σ_d, which incorporates the Rutherford cross section as well as the amount of transferred energy (equation 6), is very high due to significantly higher value of E_T for hydrogen (Figure 2c). A divergent behaviour of C-H and C-C bonds in the most useful range of e-beam energies (Figure 2d) implies that there are no feasible TEM conditions in which a molecule containing both C-H and C-C could remain unaffected by the e-beam. Therefore, aiming for lowest possible energies of the e-beam for imaging organic molecules may be counterproductive as, in fact, the $\sigma_d(E)$ for a C-H bond subsides to a moderate value at E > 80 keV, due to the lower σ_R of such a small nucleus with faster electrons, so that the use of an intermediate E ~80-

120 keV, where both C-C and C-H bonds have moderate, finite stability (Figure 2c), may present a compromise for studying the structures of organic molecules.

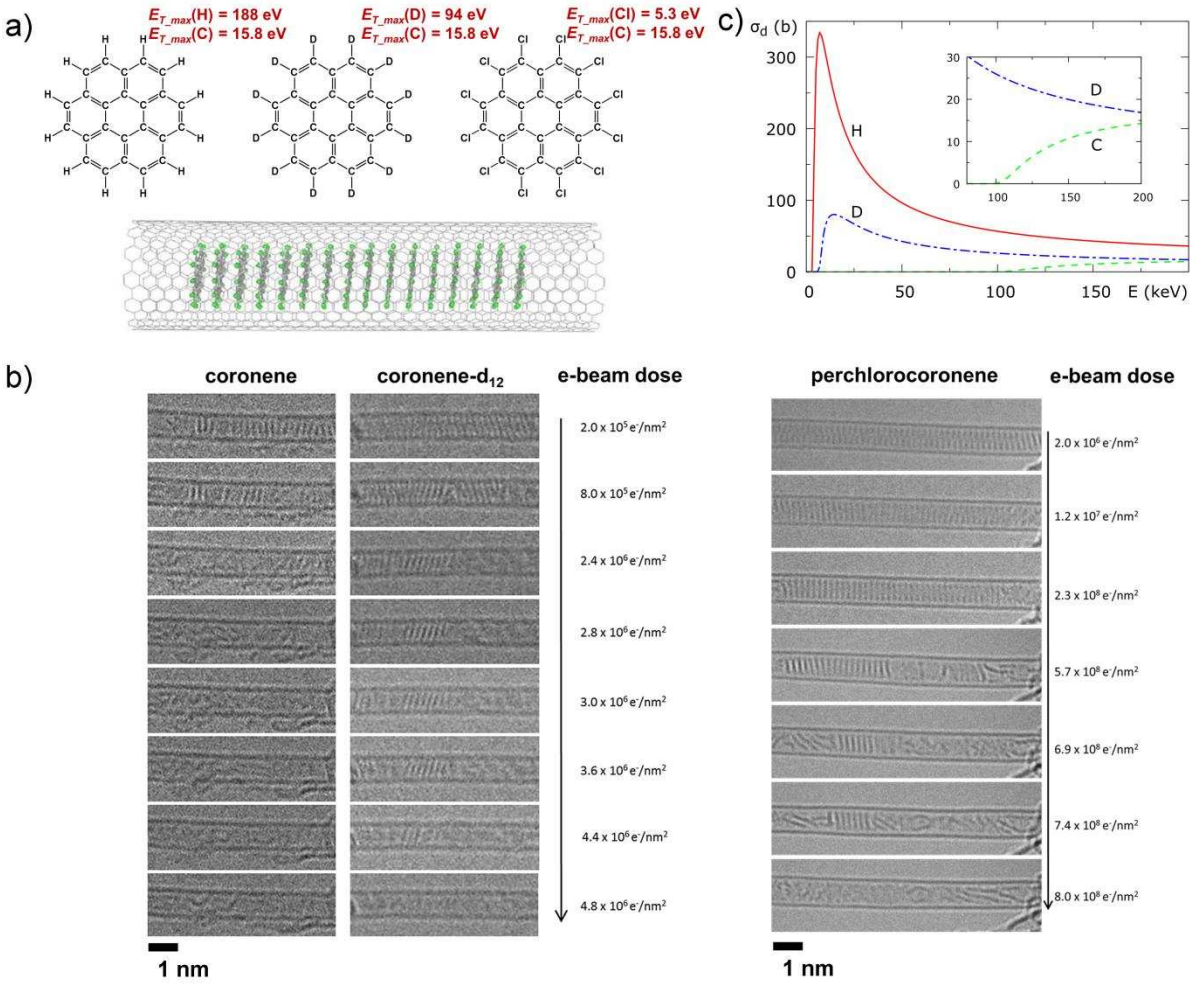

Figure 3. (a) Polyaromatic molecules form stacks in nanotubes where each molecule appears as a distinct vertical line, and the amount of energy transferred from the 80 keV e-beam is determined by the composition of the molecule. (b) Replacing all H-atoms in coronene for deuterium or Cl-atoms reduces the amount of transferred energy thus improving the stability of molecules under the 80 keV e-beam. (c) Cross section, σ_d, quantifies the difference in stabilities of C-H and C-D bonds in the e-beam.

Owing to the fact that protium (H) and deuterium (D) have the same atomic charge (Z = 1) but the atomic weight (m_n) of D is twice that of H, the above rationale for C-H bond behaviour in TEM can be verified by comparing experimentally measured lifetimes (t) of coronene ($C_{24}H_{12}$) and deuterated coronene ($C_{24}D_{12}$) as functions of the dose rate (j) of the 80 keV e-beam (Figure 3a). Because t and j are linked via the cross section, σ_d, of C-H bond dissociation (equation 3), the observed lifetime (i.e. inverse of the reaction rate) of $C_{24}D_{12}$ is increased by a factor of 2.4 [6]. Importantly, replacement of all hydrogen atoms in coronene with much heavier atoms than deuterium, such as chlorine atoms in perchlorocoronene $C_{24}Cl_{12}$ (PCC), drastically enhances the stability of the molecule, by a factor of ~1000, such that any measurable transformations of PCC can be detected only at a very high dose of the 80 keV e-beam (Figure 3b) [7]. These experiments prove that the lack of stability of the C-H bond originates mainly from the exceptionally low atomic weight of hydrogen that is posing a significant challenge to studying organic molecules by TEM.

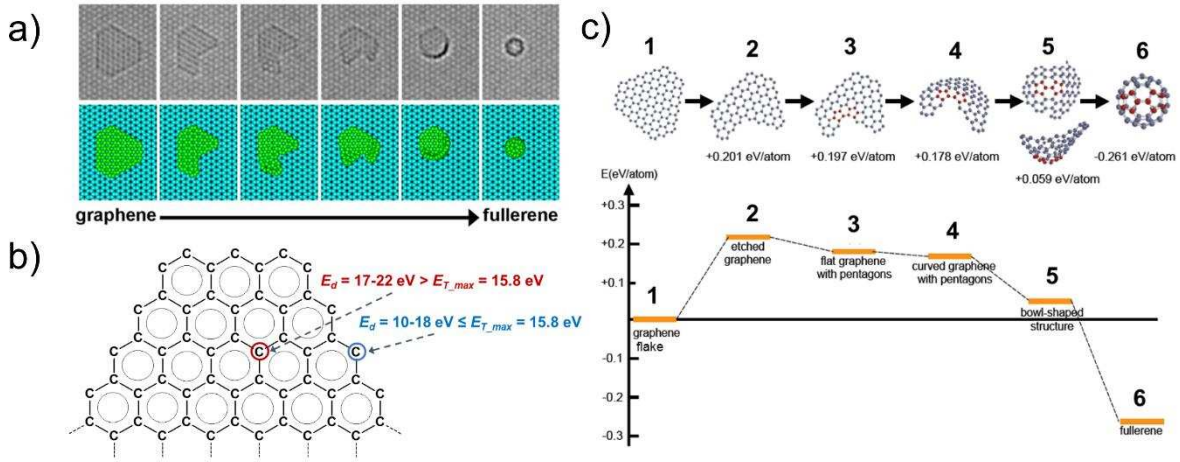

Figure 4. (a) Transformation of a graphene flake to fullerene driven by the 80 keV e-beam is based on a difference of threshold energies, E_d, for carbon atoms with three and two bonds (b), such that C-atoms are removed by the e-beam from the edge of the flake (c) leading to the formation of pentagons required for the fullerene structure.

Reactions on graphene

The scene is now set for *ChemTEM* to explore examples of specific molecules, from our previous work, using the e-beam of the TEM not as a passive 'observer' but as a very active stimulus promoting different reactions in the molecules while continuously imaging them. Firstly, the specimen must be very thin such that each incident electron of the e-beam interacts only once with the molecule, thus ensuring that transformations are driven by kinetic energy of the e-beam transferred directly to the atom (equations 2-6). Molecules supported on graphene substrate, which can also serve as a sink for charge or heat, satisfy this requirement.

Molecules consisting of 100-200 sp^2-carbon atoms (graphene 'flakes') adsorbed on graphene have been shown to undergo chemical transformations in the 80 keV e-beam [8]. Continuous TEM imaging of the initially flat 'flake' showed that the molecule changes its shape over time, gradually transforming into a non-flat structure which continues evolving until it becomes a fullerene (Figure 4a). This transformation requires sequential removal of atoms from the edge of the carbon 'flake', formation of pentagons and Stone-Wales rearrangements, all of which require significant activation energy supplied by the 80 keV e-beam, which drives the formation of fullerene. Under TEM conditions a graphene 'flake' is less stable than the fullerene because the latter has no dangling bonds or edge atoms. The edge carbon atoms have a much lower E_d of 10-18 eV (hence higher σ_d and higher k) as compared to the C-atoms in the middle of the molecule (E_d = 17-22 eV), and therefore this significantly heightened reactivity of the edge carbon atoms under the 80 keV e-beam ensures the formation of the thermodynamically stable product – fullerene, a molecule with no edges.

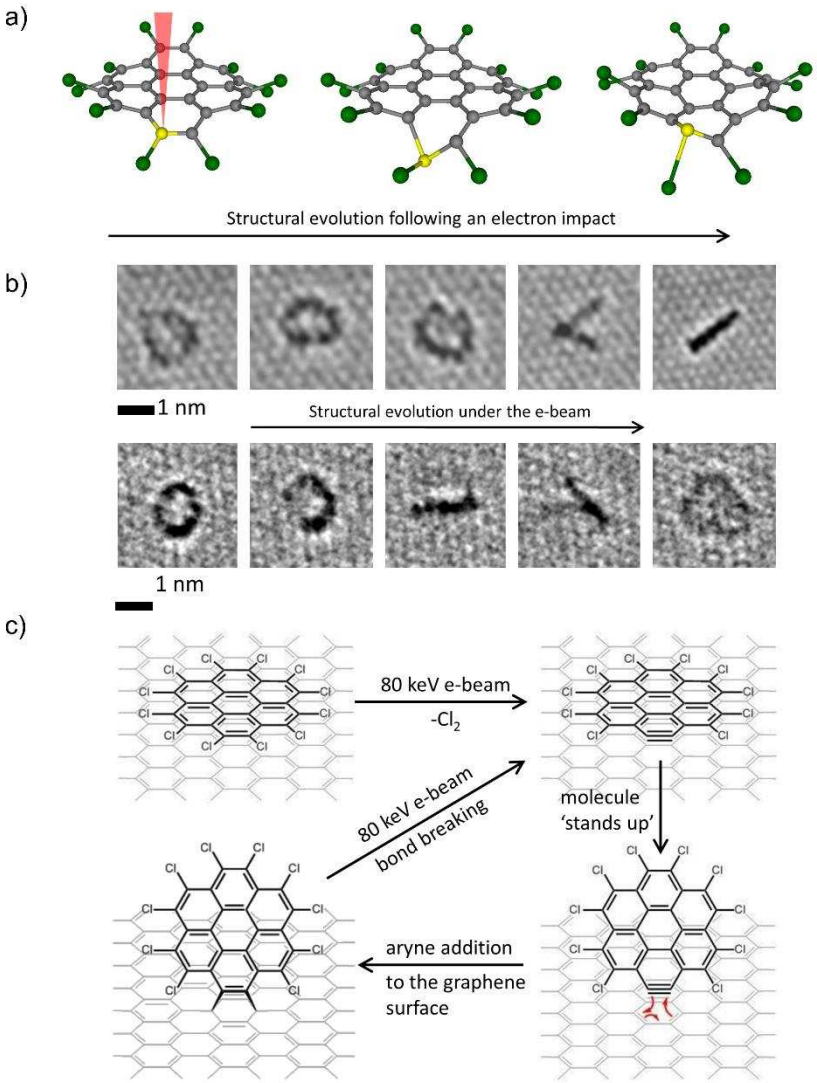

Figure 5. (a) Perchlorocoronene on graphene undergoes C-Cl bond dissociation due to impact of the 80 keV e-beam, (b, c) leading to the formation of aryne species that react with the graphene substrate thus changing orientation of the molecule from face-on to edge-on.

Under similar conditions (E = 80 keV), PCC terminated with Cl-atoms, much heavier than carbon, undergoes a slow process of Cl_2-elimination via cleavage of two C-Cl bonds by the e-beam [9]. *ChemTEM* imaging shows the molecule changing from an initial face-on to edge-on orientation (Figure 5a,b) due to Diels-Alder cycloaddition of the aryne $C_{24}Cl_{10}$ derived from PCC to graphene (Figure 5c). However, the observed cycloadduct is metastable, and therefore the aryne is released to continue further fragmentation.

Reactions in nanotubes

The low barrier for migration of physisorbed molecules on graphene is a drawback for *ChemTEM* because any molecular motion on the timescale faster than image capture will render their imaging difficult or even impossible. But carbon nanotubes can severely restrict dynamic freedom of the

guest-molecules when the molecules are densely packed in a nanotube (Figure 1), such as in C_{60}@SWNT. However, in the case of sparsely filled nanotubes [10] or flexible molecules [11] vigorous molecular motion may persist even within confines of the nanotube which limits the levels of structural information (Figure 6a).

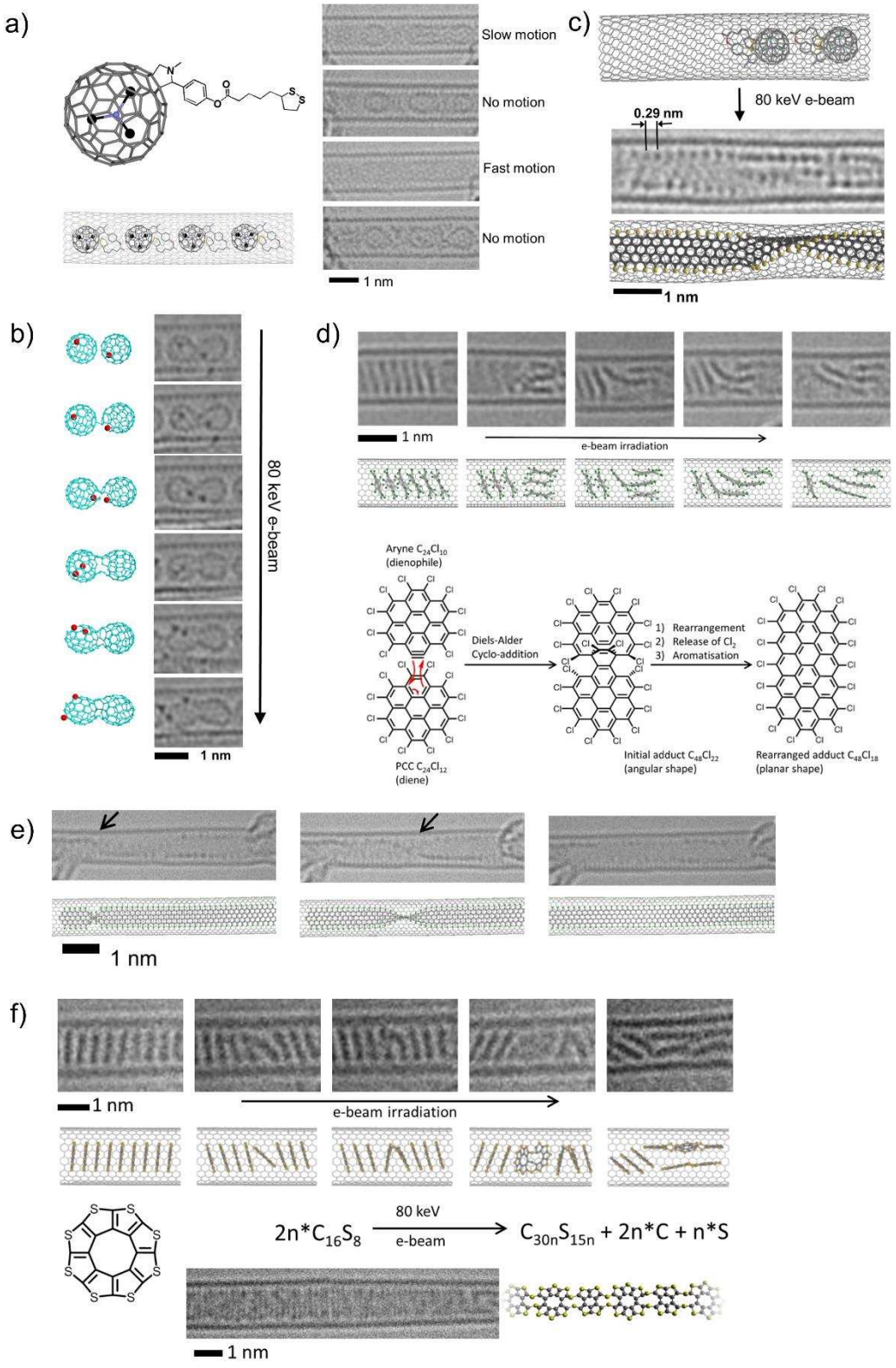

Figure 6. (a) Restricted motion of molecules in nanotubes allows accurate analysis of their structures when the molecules are stationary. (b) The 80 keV e-beam activates bonds of Dy@C_{82} fullerene, (c) thioctic ester fullerene, (d) perchlorocoronene and (f) octathiacirculene transforming them into new products, such as sulphur or chlorine terminated graphene nanoribbons (e) (black arrows indicate points of twists in the nanoribbon).

Chemical transformations of endohedral fullerene Dy@C_{82} tightly packed in SWNT can be followed with atomic precision using the same approach as on graphene [12]. Dissociation of C-C bond in the C_{82} followed by cross-linking of the carbon cages and release of Dy-atoms from the fullerene into the SWNT cavity are driven by the 80 keV e-beam (Figure 6b) while Dy-atoms appear to play an important role in promoting dissociation of the C-C bonds of the fullerene and even bonds of the host-nanotube at higher electron dose [12].

Reactions of molecules in *ChemTEM* are not necessarily limited to decomposition into poorly-defined fragments. A directional growth of graphene nanoribbons from fullerene functionalised with thioctic ester, driven by the 80 keV e-beam [13], has been demonstrated (Figure 6c). Sulphur, rather than other elements (N, O and H) available within the reactant molecule, plays a crucial role in stabilising the open edges of the nanoribbon. Because S is the heaviest element (m_n = 32) in this experiment it receives the least amount of kinetic energy from the e-beam (equation 2) making S-atoms most suitable for stabilising otherwise unstable graphene nanoribbons in *ChemTEM*. Later studies have shown that S-terminated graphene nanoribbons can be readily synthesised from other sulphur-containing molecules, either under the e-beam of TEM or via heat treatment [14,15].

Under the same conditions, perchlorocoronene $C_{24}Cl_{12}$ molecule is much less reactive, which enables imaging of the individual steps of Cl-terminated nanoribbon formation from PCC [7]. Time-series TEM images reveal all of the key steps of the reaction of polycondensation of PCC to nanoribbon, including de-chlorination followed by Diels-Alder cycloaddition of the aryne to a neighbouring PCC, rearrangement and planarization of the angular cycloadduct, ultimately leading to extended Cl-terminated polyaromatic species – the beginning of zigzag graphene nanoribbons (Figure 6d,e). Altering the composition of the reactant molecule from PCC to octothiacirculene (OTC), affects the structure of the nanoribbon formed: OTC polycondensation under the 80 keV e-beam proceeds via de-sulphurisation, cycloaddition, rearrangement and planarization – steps similar to the polycondensation of PCC, but with the final product having undulating (rather than straight zigzag) edges due to the presence of bridging S-atoms in the backbone of the nanoribbon (Figure 6f). Because S- and Cl-atoms have similar atomic weights and therefore receive a very similar amount of energy from the e-beam, comparison of PCC and OTC reactivity under the same conditions emphasises the chemical context of *ChemTEM* transformations. Stoichiometry of the reacting elements is equally important in *ChemTEM*, as the sulphur-containing nanoribbon derived from OTC is structurally different from the sulphur-terminated zigzag nanoribbon derived from thioctic ester fullerene, because the ratio C:S in OTC is too low to form a continuous graphenic lattice, so that S-atoms must be incorporated in the backbone of the nanoribbon [7].

Reactions in nanotubes involving metals

ChemTEM principles of reactivity in the e-beam extend to inorganic molecules, as shown by comparison of the transformations of $[M_6I_{14}]^{2-}$ polyiodide complexes [16]. The 80 keV e-beam promotes tumbling of octahedral metal complexes $[Mo_6I_{14}]^{2-}$and $[W_6I_{14}]^{2-}$, which possess identical size and shape (Figure 7a). However, time-resolved *ChemTEM* reveals a very important difference: while $[W_6I_{14}]^{2-}$ remains chemically unperturbed by the e-beam, $[Mo_6I_{14}]^{2-}$ loses two iodide anions and

transforms into a rod-like polyiodide structure $[Mo_6I_{12}]_n$ within the nanotube (Figure 7b). Considering the similarities in Mo-I and W-I bonding, the E_d values for these bonds within the $[M_6I_{14}]^{2-}$ complex should be expected to be very similar, however a significant difference in their atomic weights (m_n(Mo)= 96, m_n(W)= 184) ensures that a substantially larger amount of energy is transferred to Mo which is sufficient to trigger elimination of iodide and polycondensation of $[Mo_6I_{14}]^{2-}$ to $[Mo_6I_{12}]_n$ whereas $[W_6I_{14}]^{2-}$remains unchanged under the same conditions [16]. Notably, some parallels between polycondensations of $[Mo_6I_{14}]^{2-}$ to $[Mo_6I_{12}]_n$ and $C_{24}Cl_{12}$ to nanoribbon become apparent: in both cases it is energy, E_T, transferred to the lighter elements (Mo or C respectively) that triggers elimination of the halogen (I or Cl respectively), which is a crucial activation step in both reactions.

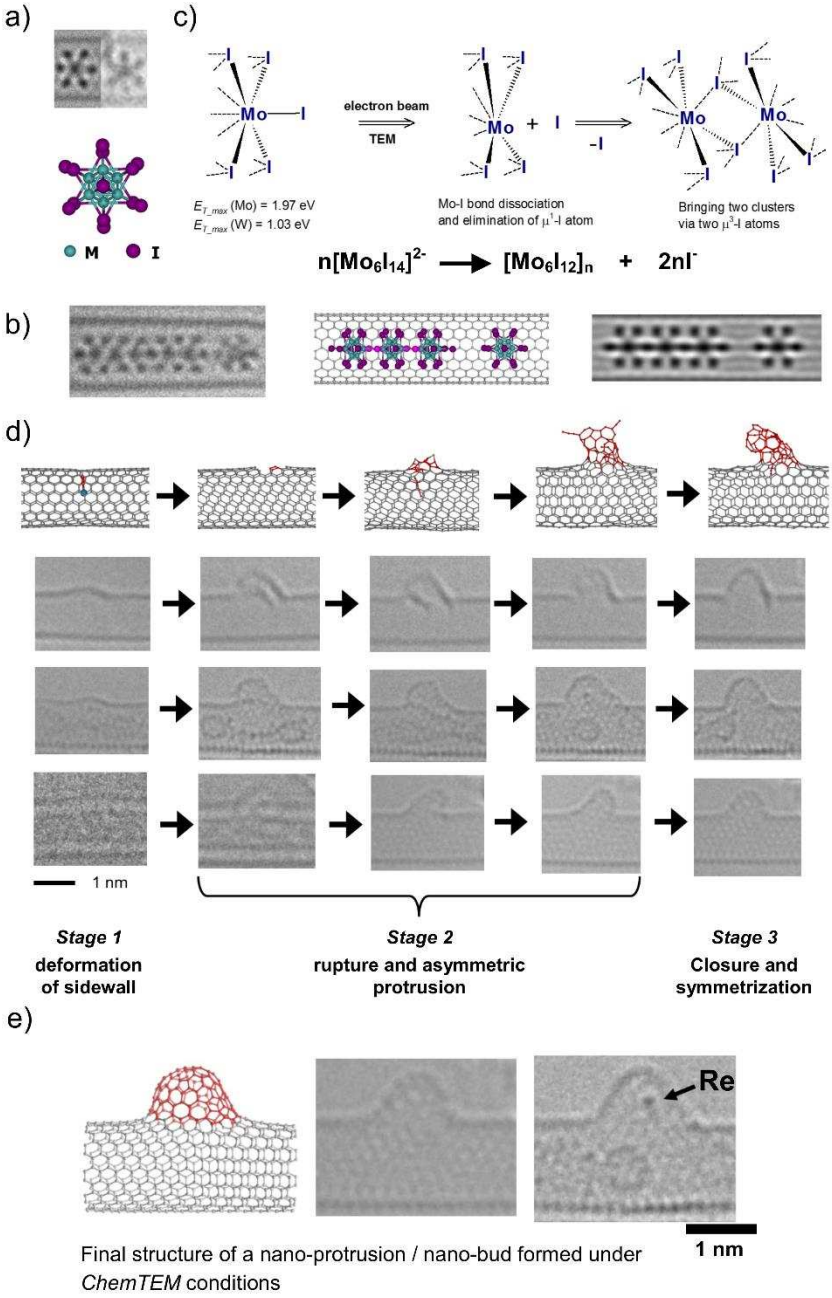

Figure 7. (a) Octahedral complexes of Mo and W polyiodides have identical structures. (b-c) However, under the 80 keV e-beam the lighter Mo-atoms receive more energy which causes Mo-I bond dissociation and polycondensation of $[Mo_6I_{14}]^{2-}$ to a polymeric phase $[Mo_6I_{12}]_n$. (d) Mechanism of nano-protrusion formation in SWNT sidewall studied by *ChemTEM*, and (e) atomic structure of a nano-protrusion ('nanobud').

Under the e-beam below 86 keV, carbon atoms of the SWNT do not receive sufficient energy to dissociate from the nanotube [17]. For example, under the 80 keV e-beam a defect-free SWNT remains unreactive ($E_{T\_max} < E_d$, and so σ_d and k are zero), but when in contact with a transition metal atom or cluster of atoms the same nanotube can undergo unexpected and dramatic chemical reactions, such as extensive defect formation promoted by Os [18] or Ni [19], or formation of a protrusion in SWNT sidewall catalysed by Re atom (Figures 7d) [20]. Metal-carbon bonding between the host-nanotube and the guest-metal perturbs the valence state of the C-atoms thus decreasing their E_d and making SWNT more reactive. The extent to which the nanotube is activated for reactions under the e-beam is strongly dependent on the position of the metal in the Periodic Table. For example, activation of C-C bonds in SWNT promoted by metal clusters was shown to increase in a triad of W-Re-Os Period 6 [18] (Figure 8a,b). Trends observed by *ChemTEM* within transition metal Groups are more complex, as for example in a triad of Fe-Ru-Os, the nature of the metal activity changes from rearrangement of carbon atoms (to form metal carbide or hemispherical carbon shells) to elimination of carbon atoms from the host-nanotube upon descending in Group 8 [21] (Figure 8d). It is important to emphasise that in all *ChemTEM* measurements on metals@nanotubes it is the energy E_T transferred to the carbon atoms that drives reactions, because transition metals have higher atomic weights hence receive significantly less energy than carbon. However, the type of metal crucially determines the rate and the type of reactions of carbon atoms.

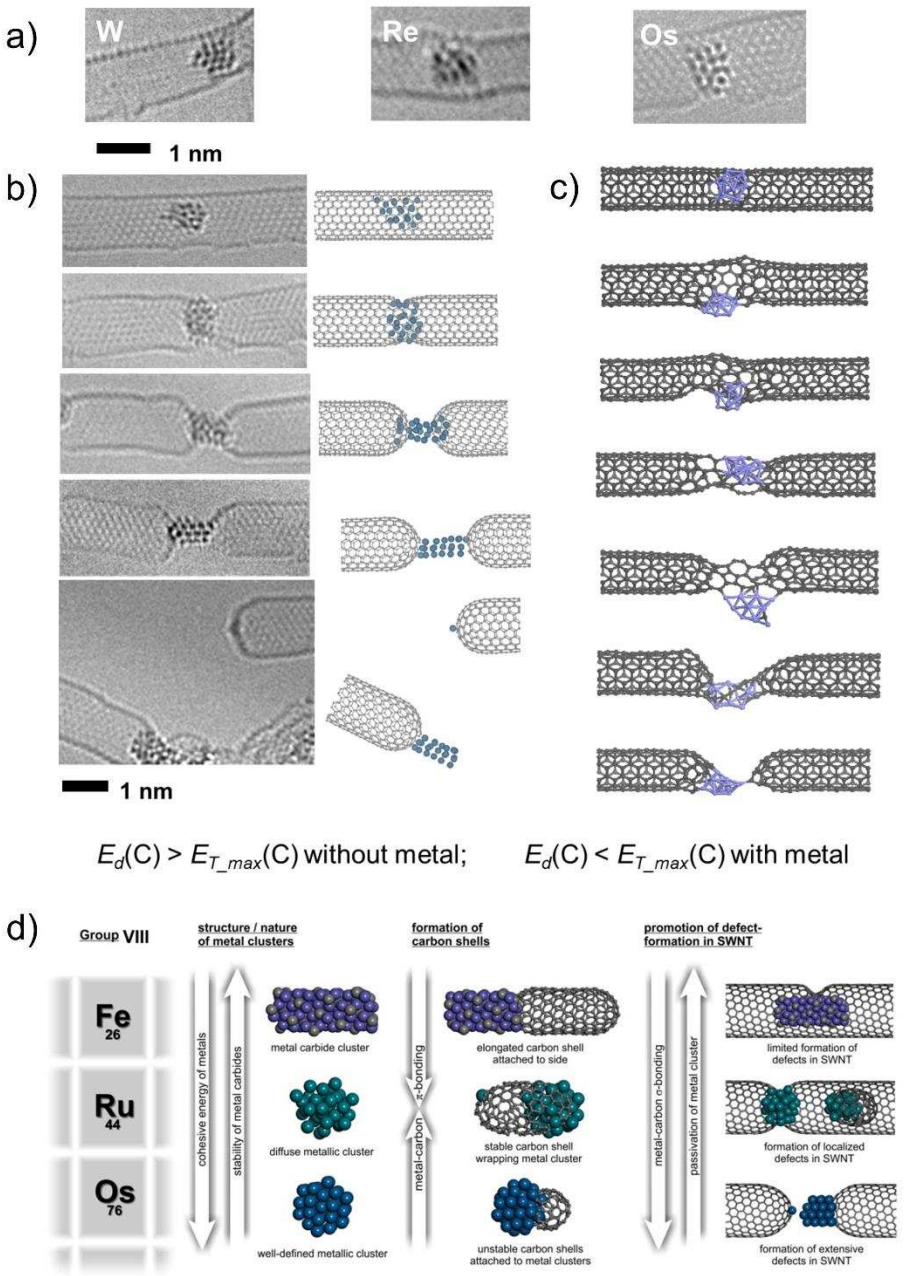

Figure 8. (a) Nanometre-sized clusters of different metals under the 80 keV e-beam catalyse different transformation in nanotubes, (b) such as extensive defect formation in the SWNT sidewall in the cases of Os@SWNT (b) or Ni@SWNT (c), because metal-carbon bonding is decreasing E_d(C). (d) Dynamics of metal-carbon interactions imaged by *ChemTEM* and compared for a group of metals are related to the catalytic properties of the metals.

Reaction rates in *ChemTEM*

All of the above examples of *ChemTEM* indicate that arranged in a chronological order time-series TEM images can form a stop-frame 'movie' of a chemical reaction, showing step-by-step transformations of reactants to intermediates to final products under the e-beam, at the single-molecule level, in direct space and in time. Remarkable examples of time-resolved imaging of

conformational changes in molecules have also been reported [22]. How can TEM imaging of reactions be possible if the temporal resolution of TEM (typically 0.1 – 1.0 seconds) is not as good as that of spectroscopy methods used for studying reactions? The key to answer this is the fact that reactions studied by *ChemTEM* are not spontaneous, and require activation via energy supplied by the e-beam, meaning that the reaction rate is principally dependent on the dose rate of electrons (equation 3; Figure 2c). In thermally activated reactions molecules moving chaotically with a Boltzmann distribution of velocities are activated by kinetic energy transferred through intermolecular collisions, such that the reaction rates are strongly dependent on the temperature of the sample (equation 7) because it is the temperature that determines the rate of successful intermolecular collisions leading to successful reactions:

$$k = a\frac{k_B T}{h}e^{-E_a/RT}$$

Equation 7

where k_B is Boltzmann's constant, h is Planck's constant, a is a transmission coefficient, E_a is the activation energy of the reaction, and R the universal gas constant.

The reaction rate constant k defined in the traditional way is a macroscopic parameter for a large ensemble of colliding molecules, whereas the reaction rate determined by *ChemTEM* is for a specific individual molecule under investigation. In *ChemTEM*, as reactant molecules are stationary, adsorbed on graphene or inside a nanotube, it is collisions with electrons of the e-beam that drive reactions. Impact of fast electrons on an atom results in one-off transfer of energy that directly triggers a reaction by shifting the atom from its equilibrium position, which is in contrast to continuous collisions that add to the average kinetic energy of the molecules (i.e. beam-induced heating over time). Therefore, it is not the Boltzmann distribution of kinetic energy of molecules but the amount and frequency of energy transfer events from the incident electrons to the atoms of the individual molecules that determine the reaction rate in TEM. Consequently in *ChemTEM* the reaction rate does not depend on temperature through Arrhenius-like equations, but instead it is almost fully controlled by the dose rate of the e-beam (equation 3) – the higher j, the more frequent the collisions between electrons and atoms and hence the faster the reaction. Therefore, slowing down a reaction by decreasing the temperature, as employed in time-resolved spectroscopy methods, is not necessary in *ChemTEM*, as the timescale of any reaction is effectively controlled by j that can be deliberately tuned to match the reaction rate to the image capture rate. Stop-frame reaction movies made in this way often reveal images of reaction intermediates moving, interacting and reacting with each other [7-9, 12, 16, 18-21], which are kinetically stabilised species separated by energy barriers from each other and from the product. Provided the barriers are sufficiently high, life-times of reaction intermediates can be sufficiently long in *ChemTEM* to elucidate exact pathways of the reactions [7,8,19,20] thus opening the door for *studying reaction mechanisms in real space at the single-molecule level*.

Conclusions

Electron beam – molecule interactions shed light on fundamental chemical properties of molecules, pathways of their reactions and the structures of their products. Despite the fact that the mechanism of reaction activation by the e-beam is different to thermal activation, reactions discovered by *ChemTEM* can already be harnessed in preparative molecular synthesis [7,14,15] or controlled growth of sub-nm metal clusters [23], leading to new materials; while analytical potential

of *ChemTEM* demonstrated for transition metals [18-21] offers a new way of studying metal-carbon bonding and catalysis at the nanoscale.

References

1. Kaiser, U.; Biskupek, J.; Meyer, J.C.; Leschner, J.; Lechner, L.; Rose, H.; Stöger-Pollach, M.; Khlobystov, A.N.; Hartel, P.; Müller, H.; Haider, M.; Eyhusen, S.; Benner, G. Transmission electron microscopy at 20kV for imaging and spectroscopy. *Ultramicroscopy* **2011**, *111*, 1239-1246.
2. Linck, M.; Hartel, P.; Uhlemann, S.; Kahl, F.; Müller, H.; Zach, J.; Haider, M.; Niestadt, M.; Bischoff, M.; Biskupek, J.; Lee, Z.; Lehnert, T.; Börrnert, F.; Rose, H.; Kaiser, U. Chromatic aberration correction for atomic resolution TEM imaging from 20 to 80 kV, *Phys. Rev. Let.* **2016**, *117*, 076101.
3. Wu, B.; Neureuthe, A.R. Energy deposition and transfer in electron-beam lithography. *J. Vac. Sci. Technol. B.* **2001**, *19*, 2508-2511.
4. A. H. Zewail, J. M. Thomas, '4D Electron Microscopy: Imaging in Space and Time', Imperial College Press, **2009**, London.
5. Skowron, S. T.; Lebedeva, I. V.; Popov, A. M.; Bichoutskaia, E. Approaches to modelling irradiation-induced processes in transmission electron microscopy. *Nanoscale*, **2013**, *5*, 6677.
6. Chamberlain, T.W.; Biskupek, J.; Skowron, S.T.; Bayliss, P.A.; Bichoutskaia, E.; Kaiser, U.; Khlobystov, A.N. Isotope substitution extends the lifetime of organic molecules in transmission electron microscopy. *Small* **2015**, *11*, 622-629
7. Chamberlain, T.W.; Biskupek, J.; Skowron, S.T.; Markevich, A. V.; Kurasch, S.; Reimer, O.; Walker, K. E.; Rance, G. A.; Feng, X.; Müllen, K.; Turchanin, A.; Lebedeva, M. A.; Majouga, A.G.; Nenajdenko, V. G.; Kaiser, U.; Besle, E.; Khlobystov, A. N. Stop-frame filming and discovery of reactions at the single-molecule level by transmission electron microscopy. *ACS Nano* **2017**, *11*, 2509-2520.
8. Chuvilin, A.; Kaiser, U.; Bichoutskaia, E.; Besley, N.A.; Khlobystov, A.N. Direct transformation of graphene to fullerene. *Nature Chem.* **2010**, *2*, 450-453.
9. Markevich, A.; Kurasch, S.; Lehtinen, O.; Reimer, O.; Feng, X.L.; Mullen, K.; Turchanin, A.; Khlobystov, A.N.; Kaiser, U.; Besley, E. Electron beam controlled covalent attachment of small organic molecules to graphene. *Nanoscale* **2016**, *8*, 2711-2719.
10. Khlobystov, A.N.; Porfyrakis, K.; Kanai, M.; Britz, D.A.; Ardavan, A.; Dennis, T.J.S.; Briggs, G.A.D. Molecular motion of iCeC82 inside single-walled carbon nanotubes. *Angew. Chem. Int. Ed.* **2004**, *43*, 1386-1389.
11. Gimenez-Lopez, M.C.; Chuvilin, A.; Kaiser, U.; Khlobystov, A.N. Functionalised endohedral fullerenes in carbon nanotubes. *Chem. Commun.* **2011**, *47*, 2116-2118.
12. Chuvilin, A.; Khlobystov, A.N.; Obergfell, D.; Haluska, M.; Yang, S.; Roth, S.; Kaiser, U. Observations of chemical reactions at the atomic scale: dynamics of metal-mediated fullerene coalescence and nanotube rupture. *Angew. Chem. Int. Ed.* **2010**, *49*, 193-196.
13. Chuvilin, A.; Bichoutskaia, E.; Gimenez-Lopez, M.C.; Chamberlain, T.W.; Rance, G.A.; Kuganathan, N.; Biskupek, J.; Kaiser, U.; Khlobystov, A.N. Self-assembly of a sulphur-terminated graphene nanoribbon within a single-walled carbon nanotube. *Nature Mater.* **2011**, *10*, 687-692.
14. Chamberlain, T.W.; Biskupek, J.; Rance, G.A.; Chuvilin, A.; Alexander, T.J.; Bichoutskaia, E.; Kaiser, U.; Khlobystov, A.N. Size, structure, and helical twist of graphene nanoribbons controlled by confinement in carbon nanotubes. *ACS Nano* **2012**, *6*, 3943-3953.
15. Pollack, A.; Alnemrat, S.; Chamberlain, T.W.; Khlobystov, A.N.; Hooper, J.P.; Osswald, S. Electronic property modification of single-walled carbon nanotubes by encapsulation of sulfur-terminated graphene nanoribbons. *Small*, **2014**, *10*, 5077-5086.
16. Botos, A.; Biskupek, J.; Chamberlain, T.W.; Rance, G.A.; Stoppiello, C.S.; Sloan, J.; Liu, Z.; Suenaga, K.; Kaiser, U.; Khlobystov, A.N. Carbon nanotubes as electrically active nanoreactors for multi-step inorganic synthesis: sequential transformations of molecules to nanoclusters and nanoclusters to nanoribbons. J. Am. Chem. Soc. **2016**, *138*, 8175−8183.
17. Smith, B.W.; Luzzi, D.E. Electron irradiation effects in single wall carbon nanotubes. *J. Appl. Phys.* **2001**, *90*, 3509-3515.

18. Zoberbier, T.; Chamberlain, T.W.; Biskupek, J.; Navaratnarajah,K.; Eyhusen, S.; Bichoutskaia, E.; Kaiser, U.; Khlobystov, A.N. Interactions and reactions of transition metal clusters with the interior of single-walled carbon nanotubes imaged at the atomic scale. *J. Am. Chem. Soc.* **2012**, *134*, 3073-3079.
19. Lebedeva, I.V.; Chamberlain, T.W.; Popov, A.M.; Knizhnik, A.A.; Zoberbier, T.; Biskupek, J.; Kaiser, U.; Khlobystov, A.N. The atomistic mechanism of carbon nanotube cutting catalyzed by nickel under an electron beam. *Nanoscale* **2014**, *6*, 14877-14890.
20. Chamberlain, T.W.; Meyer, J.C.; Biskupek, J.; Leschner, J.; Santana, A.; Besley, N.A.; Bichoutskaia, E.; Kaiser, U.; Khlobystov, A.N. Reactions of the inner surface of carbon nanotubes and nanoprotrusion processes imaged at the atomic scale. *Nature Chem.* **2011**, *3*, 732-737.
21. Zoberbier, T.; Chamberlain, T.W.; Biskupek, J.; Suyetin, M.; Majouga, A.G.; Besley, E.; Kaiser, U.; Khlobystov, A.N. Investigation of the interactions and bonding between carbon and Group VIII metals at the atomic scale. *Small* **2016**, *12*, 1649-1657.
22. Nakamura, E.; Atomic-resolution transmission electron microscopic movies for study of organic molecules, assemblies, and reactions: the first 10 years of development. *Acc. Chem. Res*. **2017**, DOI: 10.1021/acs.accounts.7b00076.
23. Chamberlain, T.W.; Zoberbier, T.; Biskupek, J.; Botos, A.; Kaiser, U.; Khlobystov, A.N. Formation of uncapped nanometre-sized metal particles by decomposition of metal carbonyls in carbon nanotubes. *Chem. Sci.* **2012**, *3*, 1919-1924.

Biographical information

Steve Skowron was awarded his MSci degree in Chemistry (University of Nottingham), and his PhD under the supervision of Prof. Besley in the computational nanoscience group. He is currently continuing his work in the same group as a postdoctoral research fellow, studying electron-beam induced reactions in low dimensional nanomaterials.

Thomas Chamberlain obtained his PhD in Chemistry (University of Nottingham) and studied carbon nanotubes in Prof. Khlobystov's group. Currently he holds University Academic Fellowship at the University of Leeds, where his group combines fullerene based synthesis, supramolecular assembly and nanomaterial fabrication with flow chemistry for sustainable heterogeneous catalysis systems.

Johannes Biskupek is Postdoctoral Researcher in Electron Microscopy Group of Materials Science, University of Ulm. He specialises in low-voltage TEM imaging of nanomaterials.

Elena Besley is Professor of Theoretical and Computational Chemistry at the University of Nottingham. Her research interests include the development of theoretical and computational approaches to prediction of materials properties, electrostatic interactions at the nanoscale, gas storage and interactions in porous solids.

Ute Kaiser is Professor of Electron Microscopy for Materials Science, University of Ulm, and Scientific Project Leader of the SALVE III project (www.salve-project.de). She develops innovative methodologies and instrumentation for low-voltage TEM imaging of a wide range of materials.

Andrei Khlobystov is Professor of Nanomaterials at the University of Nottingham (www.nottingham.ac.uk/nanocarbon) and director of the Nanoscale & Microscale Research Centre (*nmRC*; www.nottingham.ac.uk/nmrc). He studies reactions of molecules at nanoscale and develops fundamental science of nanoreactors.

{WORD COUNT = 5968}

Reactions in *ChemTEM*